



HAL
open science

When translation elongation is impaired, the mRNA is uniformly destabilized by the RNA degradosome, while the concentration of mRNA is altered along the molecule

Marie-Pierre Duviau, Fan Chen, Anthony Emile, Muriel Coccagn-Bousquet,
Laurence Girbal, Sébastien Nouaille

► To cite this version:

Marie-Pierre Duviau, Fan Chen, Anthony Emile, Muriel Coccagn-Bousquet, Laurence Girbal, et al.. When translation elongation is impaired, the mRNA is uniformly destabilized by the RNA degradosome, while the concentration of mRNA is altered along the molecule. *Nucleic Acids Research*, In press, 10.1093/nar/gkad104 . hal-04012706

HAL Id: hal-04012706

<https://hal.science/hal-04012706>

Submitted on 3 Mar 2023

HAL is a multi-disciplinary open access archive for the deposit and dissemination of scientific research documents, whether they are published or not. The documents may come from teaching and research institutions in France or abroad, or from public or private research centers.

L'archive ouverte pluridisciplinaire **HAL**, est destinée au dépôt et à la diffusion de documents scientifiques de niveau recherche, publiés ou non, émanant des établissements d'enseignement et de recherche français ou étrangers, des laboratoires publics ou privés.

When translation elongation is impaired, the mRNA is uniformly destabilized by the RNA degradosome, while the concentration of mRNA is altered along the molecule

Marie-Pierre Duviau[†], Fan Chen[†], Anthony Emile, Muriel Coccagn-Bousquet*, Laurence Girbal* and Sébastien Nouaille^{✉*}

TBI, Université de Toulouse, CNRS, INRAE, INSA, Toulouse, France

Received May 17, 2022; Revised January 30, 2023; Editorial Decision February 02, 2023; Accepted February 09, 2023

ABSTRACT

mRNA sits at the crossroads of transcription, translation and mRNA degradation. Many questions remain about the coupling of these three processes in *Escherichia coli* and, in particular, how translation may have an effect on mRNA degradation and transcription. To characterize the interplay between mRNA degradation and translation while accounting for transcription, we altered the translation initiation or elongation and measured the effects on mRNA stability and concentration. Using a mapping method, we analysed mRNA concentration and stability at the local scale all along the transcript. We showed that a decrease in translation initiation efficiency destabilizes the mRNA and leads to a uniform decrease in mRNA concentration throughout the molecule. Prematurely terminating translation elongation by inserting a stop codon is associated with a drop in local mRNA concentration downstream of the stop codon, due to the uncoupling of transcription and translation. In contrast, this translation alteration uniformly destabilizes the coding and ribosome-free regions, in a process triggered by RNase E activity, and its ability to form the RNA degradome. These results demonstrate how ribosomes protect mRNA molecules and highlight how translation, mRNA degradation and transcription are deeply interconnected in the quality control process that avoids unproductive gene expression in cells.

INTRODUCTION

Gene expression regulation crucially allows cells to adjust their metabolic capacities to their environments. An important hub of this process is mRNA, through its involvement in transcription, translation and degradation. Many aspects of the interplay between transcription, translation and mRNA degradation in *Escherichia coli* remain to be elucidated, in particular how mRNA degradation is affected by the other two mechanisms.

In *E. coli*, mRNA is degraded by a variety of endo- and exoribonucleases, most of whose activity and mode of action are rather well understood from a mechanistic point of view (1). mRNA degradation is generally initiated by endoribonucleolytic cleavage performed mainly by the essential endoribonuclease RNase E, and occasionally by RNase III. RNase E can form a supramolecular structure called the RNA degradosome in association with polynucleotide phosphorylase (PNPase), the RNA helicase RhlB and the glycolytic enzyme enolase (Eno) (2,3). The initial cleavage products are then degraded by multiple cycles of attack by RNase E combined with the action of 3'-exoribonucleases and oligoribonuclease at the nucleotide level (4).

The link between mRNA degradation and translation is not so simple because ribosomes can both stabilize and destabilize mRNA transcripts. The protective effect of ribosomes is highlighted by the fact that mRNA is destabilized when translation initiation is limited by mutated ribosome-binding sites (RBSs) or when transcription and translation are decoupled (5–7). These results, first demonstrated for a few RBSs (8), have since been confirmed using synthetic libraries of RBSs and translation initiation regions (9,10). mRNA molecules are also destabilized by fast ribosome trafficking through the translation initiation region, which reduces ribosome coverage (11). The protective effect of

*To whom correspondence should be addressed. Tel: +33 561 55 94 38; Fax: +33 561 55 94 00; Email: sebastien.nouaille@insa-toulouse.fr

Correspondence may also be addressed to Laurence Girbal. Email: girbal@insa-toulouse.fr

Correspondence may also be addressed to Muriel Coccagn-Bousquet. Email: coccagn@insa-toulouse.fr

[†]The authors wish it to be known that, in their opinion, the first two authors should be regarded as Joint First Authors.

ribosomes on transcripts may stem from ribosomes preventing RNase E from accessing the 5' end. During translation elongation, in contrast, slowly elongating or stalled ribosomes are associated with transcript destabilization (5,6). Large-scale studies of the correlation between codon bias and mRNA stability have also shown that less optimized codons, with slowly elongating ribosomes, are associated with less stable RNAs (12,13). The reported physical interaction between the RNA degradosome and 70S ribosomes and polysomes suggests that the RNA degradosome might act as an antenna on the inner cytoplasmic membrane that captures the ribosomes (14). In addition, a recent study has shown that the clustering of degradosomes on the inner membrane depends on the presence of translationally active polysomes, with these sites possibly being involved in initiating degradation of actively translated mRNAs (15). Furthermore, when RNase E is delocalized from the membrane, this leads to an increase in ribosome-free mRNA turnover (16). These results raise questions about how mRNA degradation and quality control depend on the translational state of the molecules.

Another unanswered question is how the coupling of mRNA degradation and translation relates to transcription. On the one hand, translation is known to interact with transcription through pioneer ribosomes, which are involved in direct and indirect physical associations with RNA polymerase (17–19) and whose acceleration or deceleration alters the speed of RNA polymerase transcription (20–22). On the other hand, the coupling of transcription and translation may be limited by the different subcellular locations of transcription and translation: RNA polymerase synthesizes mRNA molecules in the nucleoid while most mRNA molecules in translation are outside the nucleoid (23). Furthermore, recent results showing that increasing the mRNA concentration by increasing transcription increases translation efficiency and decreases mRNA stability (24,25) indicate that transcription affects the regulation of mRNA degradation and translation. The dependency of translation efficiency and mRNA stability on mRNA concentration has also been observed in genome-wide correlation analyses (13,25–28). The underlying mechanism may be binding competition between mRNAs for a finite pool of RNase E (29) or ribosomes; however, the interplay between translation and transcription on the one hand, and mRNA degradation on the other, appears to be more complicated than ribosomes forming a simple steric barrier against RNase attack.

To better understand the interaction between mRNA degradation and translation while also accounting for transcription, we measured the effects on mRNA stability and concentration of modulating translation initiation or elongation. To acquire data on local variations in concentration and stability along the entire mRNA molecule, a mapping strategy based on quantitative real-time polymerase chain reaction (qRT-PCR) measurements was applied (7). A decrease in the efficiency of translation initiation was observed to destabilize mRNA homogeneously throughout the molecule, in keeping with the overall decrease in mRNA concentration. mRNA was also uniformly destabilized throughout the molecule when translational elongation was terminated prematurely. This destabilization was

driven by the presence of a ribosome-free region of mRNA and depends on RNase E activity and its ability to form the RNA degradosome. The observed decrease in local mRNA concentrations downstream of the inserted stop codon is consistent with premature termination of transcription following an uncoupling of translation and transcription. These results shed new light on how ribosomes protect mRNAs and highlight how the deep interaction between translation, mRNA degradation and transcription provides a quality control mechanism to avoid unproductive gene expression in cells.

MATERIALS AND METHODS

Bacterial growth and induction conditions

All plasmid constructs were transferred from *E. coli* DH5 α (New England Biolabs) into an MG1655 derivative (MET345) lacking *lacZ* (25). The *E. coli* strains were grown in Luria–Bertani (LB) broth for cloning, at 37°C with shaking. The cultures for RNA, polysome and protein analyses were performed in M9 minimal medium supplemented with 3 g/l glucose at 37°C with shaking (30). Ampicillin was added at 100 μ g/ml and chloramphenicol at 20 μ g/ml. RNase E mutant strains were obtained by introducing plasmids carrying *wt-lacZ* or *lacZ-Stop*_{50%} into MC1061 derivative strains containing control RNase E (RNase E wt) or the thermosensitive variant of RNase E (RNase E Ts) (31), and into KSL2000 derivative strains expressing control RNase E (RNase E wt), RNase E lacking the C-terminal region (RNase E Δ Cter) and RNase E lacking the membrane-targeted sequence (RNase E Δ MTS) (32).

LacZ mRNA transcription under the P_{BAD} promoter was induced as follows: fresh M9 medium was inoculated at OD₆₀₀ = 0.1 from an overnight culture. At OD₆₀₀ = 0.6, arabinose (Sigma) was added at a final concentration of 0.0001% and the culture was induced for 30 min. Thermosensitive RNase E mutants were grown at 30°C in M9 supplemented with 0.1% casamino acids (Difco). To evaluate mRNA degradation kinetics, transcription was arrested by adding rifampicin at a final concentration of 500 μ g/ml. Samples corresponding to 6 mg (dry weight) of cultured cells were collected at 0 min (before adding rifampicin), and at five time points covering the first 7.5 min after rifampicin addition. Samples were flash-frozen in liquid nitrogen. For RNase E thermosensitive mutants, the procedure was identical except that cultures were shifted at 42°C for 10 min before rifampicin addition. The mRNA concentrations were quantified from RNAs extracted before rifampicin addition. For the polysome profiling experiments, transcription was induced by adding arabinose [0.0001% (w/v)] at an OD₆₀₀ of 1 for 30 min, and translation was then arrested by adding 0.1 mg/ml chloramphenicol.

Construction of vectors

General DNA manipulation procedures were performed as described (33). Plasmid DNA was isolated using the QI-Aprep Miniprep Kit (Qiagen). All plasmids containing *lacZ* used in this study were derived from the pBAD-*lacZ*-myc-his plasmid (Life Science). PCRs were performed using

Phusion polymerase (New England Biolabs). Constructs were prepared by PCR assembly to replace the Shine–Dalgarno (SD) sequence and delete the untranslated regions (UTRs) of the *lacZ* coding sequence (CDS). Amplifications were gel-purified (Qiagen Gel purification kit), and the 5' ends were phosphorylated with 15 U of T4 polynucleotide kinase (New England Biolabs) for 30 min at 37°C and self-ligated with 30 U of T4 DNA ligase (New England Biolabs) at 16°C overnight. Stop codons were inserted at different positions of the *lacZ* CDS by amplifying the vector with a pair of complementary primers containing a TAG codon. After purification, *E. coli* was amplified and clones were selected by blue/white screening on plates containing X-Gal (Sigma). The orthogonal tRNA (tRNA_o) in the pEVOL plasmid was deleted by amplification of the full vector minus the tRNA portion, followed by purification, phosphorylation and self-ligation as described above. The tRNA_o was integrated in transcriptional fusion with *lacZ* by PCR. Two primers were used, which contained half of the tRNA_o while the other part hybridized with the integration site. The primers were used to amplify the whole plasmid, and the product was self-ligated. All transcriptional units constructed in this study contain the *rrnB* transcriptional terminator. All constructs were verified by sequencing (Eurofins). All primers used in this study are listed in Supplementary Table S1.

Polysome profiling

Polysome profiling experiments were performed as previously described (24). Briefly, cells were harvested after translation arrest, washed twice and resuspended in lysis buffer [20 mM Tris–HCl pH 8, 140 mM KCl, 40 mM MgCl₂, 0.5 mM dithiothreitol (DTT), 100 µg/ml chloramphenicol, 1 mg/ml heparin, 20 mM EGTA, 1% Triton X-100]. After mechanical cell disruption with glass beads, mRNA–ribosome complexes were size-separated on a sucrose gradient [10–50% (w/v) in polysome gradient buffer (the same composition as the lysis buffer except for heparin at a final concentration of 0.5 mg/ml and without Triton X-100)] into 24 subfractions. The levels of 16S and 23S rRNAs in each subfraction were calculated using a 2100 Bioanalyzer (Agilent, Santa Clara, CA, USA) and used to pool the mRNA into seven fractions labelled A–G. Fraction A consisted of free mRNA molecules not undergoing translation, while fractions B–G consisted of mRNA copies in translation bound to increasing numbers of ribosomes (one bound ribosome in fraction B to ~11 bound ribosomes in fraction G) (24). Protein denaturation and nucleic acid precipitation were performed in the pooled subfractions as previously described (28).

RNA extraction, quality control and cDNA synthesis

Total RNA was extracted using RNeasy mini extraction kits (Qiagen) according to the manufacturer's recommendations in a Qiacube robot (Qiagen). Before cell lysis, each sample was centrifuged for 10 min at 8000 rpm at 4°C, resuspended in 500 µl of RLT buffer and transferred into a tube containing 0.1 g of glass beads. The cells were disrupted at 4°C in three 30 s cycles using a FastPrep-24 instrument (MP

Biomedicals). After 10 min centrifugation at 4°C and 13 000 rpm, 350 µl of supernatant was purified in a Qiacube robot (Qiagen). Total RNA was eluted in 50 µl of elution buffer. Any residual genomic DNA contamination was removed by additional DNase treatment. Total RNA samples (50 µg) were treated with 2 U of Turbo-DNase (Ambion) for 15 min at room temperature followed by an RNA clean-up using an RNeasy Mini Kit (Qiagen). The absence of significant genomic DNA contamination was checked by qPCR. RNA concentrations were measured by UV–visible light spectrophotometry (ND-1000, NanoDrop Technologies) and the integrity of the molecules was confirmed using a 2100 Bioanalyzer (RIN >8.5) with the RNA 6000 Nano LabChip kit (Agilent). The RNAs were stored at –80°C until use.

cDNA was synthesized from 5 µg of total RNA using SuperScript II reverse transcriptase (1.5 U, Life Technologies) as previously described (34). For each fraction of the polysome profiling experiments, an equal amount of Ambion™ ERCC RNA Spike-In mix was added to a constant amount of total RNA (0.2 µl of ERCC RNA mix diluted 1:100 for 1 µg of total RNA) before retro-transcription. The cDNAs were serially 10-fold diluted to identify the dilution level corresponding to a cycle threshold (Ct) of between 10 and 25 for representative primer pairs targeting *lacZ* cDNA using a LightCycler 480 II real-time PCR instrument (Roche).

β-Galactosidase assay

Cells (3 mg dry weight) were collected, harvested, washed twice with ice-cold 0.2% KCl, resuspended in 1 ml of lysis buffer (15 mM Tris tricarballoylate, 4.5% glycerol, 0.9 mM MgCl₂, 0.2 mM DTT; pH 7.2), transferred into screw-capped tubes containing 0.1 g of glass beads and disrupted using a FastPrep-24 instrument (MP Biomedicals) (six 30 s cycles at 6.5 m/s with 1 min on ice in between). The supernatant containing soluble proteins was analysed immediately. All measurements were carried out on three biological replicates with six technical replicates for each.

The total protein content of the cell extracts was determined by the Bradford method with bovine serum albumin as the protein standard. β-Galactosidase activity was determined by the colorimetric method using *O*-nitrophenyl-β-D-galactopyranoside (ONPG; Sigma) as substrate. Protein activity was determined using the rate of ONP production at 30°C (measured from the absorbance at 420 nm using a SpectraMax plus spectrophotometer) and expressed as a specific activity (mmol/min/g) using the total protein concentration of the sample. For each quantification, at least two independent samples were extracted and six technical replicates were analysed at different dilutions.

Primer design for qRT-PCR and validation

Primers for qPCR (Eurofins Genomics) were designed using Vector NTI advance v11 (Life Technologies) with a melting temperature of 59–61°C, a length of 20–22 bp and a GC content of 50–67%. The reaction efficiency of each pair of primers was tested as a single amplicon on serial dilutions of pBAD-*lacZ*-*myc*-his and cDNA as a matrix, and

validated at ~100% PCR efficiency with a single amplicon. The minimum information for publication of quantitative RT-PCR experiments (MIQE) not detailed in the main text is shown in Supplementary Table S10. One set of primer pairs was designed to quantify *lacZ* (Supplementary Table S1). Amplicons are identified by a letter in the figures, indicating their position (in nucleotides) relative to the *lacZ* +1 transcriptional start site (TSS): a (113–227), b (701–831), c (861–986), d (1219–1338), e (1516–1617), f (1666–1685), g (2286–2415), h (2523–2615), i (2735–2837) and j (3223–3337). The coordinates of the different regions are as follows: 5'-UTR, 1–33; *lacZ* CDS, 34–3269; and tRNA_o, 3317–3423 (in nucleotides with respect to the +1 TSS). The housekeeping gene *ihfB* [integration host factor β -subunit (35)] and *bla* (ampicillin resistance gene carried by the plasmid) were used as internal normalization controls.

Quantitative RT-PCR

Low-throughput qRT-PCR was performed with a LightCycler 480 II device (Roche) on 96-well plates (Biorad) with SyberGreen MasterMix (Biorad). High-throughput qRT-PCR was carried out using the 96.96 dynamic array™ IFCs (integrated fluidic circuits) and the BioMark™ HD System (Fluidigm Corporation, CA, USA) following the manufacturer's protocol (36) at the Gentiane platform (Clermont Ferrand, France). Briefly, 14 pre-amplification cycles were performed with a pooled primer mixture (0.2 μ M). The pre-amplified samples were treated with 8 U of exonuclease I (New England BioLabs), diluted 5-fold with Tris-EDTA buffer and added to a 'Sample Mix' consisting of TaqMan® Gene expression Master Mix (Applied Biosystems), DNA Binding Dye Sample Loading Reagent (Fluidigm), EvaGreen® dye (Biotium) plus Tris-EDTA buffer, as recommended. In parallel, each primer pair (20 μ M) was added to a 'Primer Mix' composed of assay loading reagent (Fluidigm) plus Tris-EDTA buffer, as recommended. An IFC controller was used to prime the fluidics array, then 5 μ l of each sample and primer mix were loaded into the appropriate inlets. The loaded chip was transferred to the BioMark™ HD System and qPCR was performed using the following temperature program: 2 min at 50°C, 30 min at 70°C and 10 min at 25°C; followed by a hot start at 50°C for 2 min; then 10 min activation at 95°C for 35 PCR cycles involving 15 s at 95°C for denaturation and 60 s at 60°C for annealing and elongation. The melting curve analysis consisted of 3 s at 60°C followed by heating to 95°C with a ramp rate of 1°C/3 s. To determine the steady-state mRNA concentration, each sample was loaded 1–3 times in the array and each primer pair was loaded 2–5 times for technical replicates. mRNA decay was quantified similarly, resulting in 12–30 technical replicates for each biological sample used to measure the degradation kinetics and for each primer pair. In the polysome profiling experiment, *lacZ* mRNA abundance was quantified in duplicate using primer pair 361-LacZ/362-LacZ and ERCC 074 RNA using 785 ERCC074-786 ERCC074 (Supplementary Table S1). Raw qRT-PCR data are provided in Supplementary Tables S2–S9. We controlled that the variations in mRNA concentrations and stabilities detected in this work were not related to

the altered expression of key enzymes of the mRNA degradation machinery (Supplementary Figure S1).

Data analysis and statistical treatment

Ct values for low- and high-throughput quantification were determined with automatic baseline detection. Results for direct comparisons were expressed as fold change (FC) between strains relative to the control strain (containing *wt-lacZ*). The Pfaffl analysis method was used (37), considering Δ Ct ratios between strains exclusively for the same primer pair. Results are expressed as mean FC with standard deviations across biological and technical replicates.

To compare local *lacZ* mRNA concentrations between strains, Ct values were compared with a normalization range made with an 8-log dilution of pBAD-*lacZ* plasmid and expressed as $\Delta\Delta$ Ct after normalization by the ampicillin resistance gene carried by the plasmid to avoid any effect due to putative plasmid copy number changes between strains (37). The same results were obtained with *ihfB* normalization, confirming that the plasmid copy number was unmodified between the analysed strains. To quantify local concentration variations along one mRNA *lacZ* molecule in one strain, Ct values were compared with the pBAD-*lacZ* plasmid 8-log range and then expressed as FCs relative to the values for amplicon 'a' located at the 5' side of the mRNA ($\Delta\Delta$ Ct). We verified that the inter-strain variations of Ct values between *ihfB* and *bla* mRNAs were not significant.

To determine the mRNA half-life for each technical replicate and each primer pair, Ct values were plotted as a function of time after rifampicin addition. The mRNA half-life ($T_{1/2}$) was calculated from the degradation rate constant (k) corresponding to the slope of the Ct versus time curve with the relationship $T_{1/2} = 1/k$. Only slopes with an $R^2 > 0.85$ were considered, except for very stable mRNAs (half-lives >10 min) due to greater uncertainty in slope determination. Examples of plots used for half-life determination are presented in Supplementary Figure S2. The half-lives measured for each repetition and primer pair are expressed as means and standard deviations.

To obtain the relative *lacZ* mRNA abundance in each fraction of the polysome profiling experiments, the relative *lacZ* mRNA abundance compared with a constant quantity of the ERCC 074 RNA was calculated using the method of FC Δ Ct values (37) and normalized by the total RNA quantity extracted in each fraction. To obtain the distribution of the abundance of *lacZ* mRNA, the proportion of mRNA copies in each fraction was calculated by dividing the relative abundance in one fraction by the sum of the abundances in all the fractions (28).

Translation restoration at the internal amber stop codon

Translation restoration at the internal amber stop codon was based on the pEVOL orthogonal translation system involving an orthogonal amino acid tRNA synthetase (aaRS_o) and a tRNA_o (38). In the presence of a non-canonical amino acid, namely AzF (4-azido-L-phenylalanine, Iris Biotech GmbH, Germany) used in this study, the orthogonal aaRS_o acylates the orthogonal

tRNA_o with AzF, which is in turn used by ribosomes to decode the amber stop codon UAG and restore translation. We used a pEVOL plasmid derivative to encode aaRS_o but in which the tRNA_o was deleted. The orthogonal tRNA_o was instead inserted in transcriptional fusion with the *lacZ*-Stop_{50%} CDS to produce the *lacZ*-Stop_{50%}-tRNA_o transcript. AzF was dissolved in 1 M NaOH and added to the culture medium at a final concentration of 2 mM at the beginning of growth.

RESULTS

Reducing the efficiency of translation initiation destabilizes mRNA evenly throughout the molecule and decreases its overall concentration

To investigate the coupling between translation and mRNA degradation, we first modulated the translation initiation efficiency, using the *lacZ* mRNA coding for β -galactosidase carried by a plasmid as a reporter. The wild-type version is composed of a 3267 nt long CDS and a 33 nt 5'-UTR sequence containing the close-to-optimal SD sequence, AG-GAGG, to sustain efficient translation initiation (39). To make translation initiation less efficient, we recoded the SD sequence to TTATAA (*SD-lacZ*, Figure 1A). The amount of β -galactosidase produced with the inefficient SD was ~ 10 times lower than with the reference SD (Figure 1B). Figure 1C shows that for *wt-lacZ*, with efficient translation initiation, the majority of *lacZ* mRNAs were in the more heavily ribosome-loaded fractions (F and G), with >8 bound ribosomes. Only a small proportion of *wt-lacZ* mRNAs were free of ribosomes (fraction A). These results show that almost all *wt-lacZ* mRNAs were being translated and were loaded with multiple ribosomes. The proportion of *SD-lacZ* mRNAs loaded with >10 ribosomes (fraction G) was significantly lower while the proportions of mRNAs loaded with just a few ribosomes (fractions B, D, E and F) or without ribosomes (fraction A) were significantly higher. These results show that reducing the efficiency of translation initiation decreased the proportion of translated *lacZ* mRNAs and reduced the number of loaded ribosomes on those in translation.

We then measured the effects of a decrease in translation initiation efficiency on the stability and concentration of *lacZ* mRNA. mRNA is typically quantified using northern blots with a single probe or by qRT-PCR with one amplicon. Both only provide partial information because they target only one part of the analysed molecule. Here we used a more comprehensive qRT-PCR approach at the molecular scale to measure local concentrations and local stabilities throughout the *lacZ* mRNA molecule (7). In this study, we define 'local concentration' as the concentration of a region of *lacZ* mRNA measured by a pair of primers in steady state. Similarly, we define 'local stability' as the half-life of a region of the *lacZ* mRNA measured by a pair of primers, during RNA decay after transcription arrest by rifampicin. Sets of primer pairs distributed throughout the molecule, from the 5' to the 3' end, were designed to map the behaviour of different portions of the mRNA molecule (for amplicon boundary locations, see the Materials and Methods). Although this methodology did not distinguish between full-length mRNA and fragments of mRNA, this

approach allowed us to identify local differences between constructs.

The local half-lives of *wt-lacZ* and *SD-lacZ* (Figure 2B) were quantified at eight different mRNA locations (Figure 2A). The stability of *wt-lacZ* varied little across the molecule, with local half-lives ranging from 2.8 to 2.2 min and an average half-life of 2.4 min (Figure 2C). The stability of *SD-lacZ* mRNA was likewise similar throughout the molecule, but with half-lives reduced by $>50\%$ compared with *wt-lacZ* (Figure 2B, C). It was already known that reduced translation efficiency destabilizes *lacZ* mRNA (8); here we showed that this destabilization is uniform along the *lacZ* mRNA. Figure 2D shows the effects of reducing the efficiency of translation initiation on local mRNA concentrations throughout the molecule. Changes in local mRNA concentrations are expressed as intramolecular FCs relative to the 5' end of the molecule (using amplicon 'a'). No significant variations across the molecule were observed either for *wt-lacZ* or for *SD-lacZ*. The average transcript concentration was $\sim 60\%$ lower for *SD-lacZ* than for *wt-lacZ* (Figure 2E). This uniform decrease in mRNA concentrations is similar in scale to the level of destabilization observed for *SD-lacZ* mRNA (i.e. a decrease of $\sim 50\%$). Since the concentration of mRNA is determined by the balance of synthesis via transcription and degradation, this suggests that transcription is not strongly modified under these conditions.

In summary, reducing the efficiency of translation initiation reduced the stability and concentration of *lacZ* mRNAs, and reduced their ribosome loading, with all these effects contributing to reduced synthesis of β -galactosidase protein. Furthermore, the decrease in concentration and stability was uniform throughout the molecule. The nearly constant half-lives measured throughout the molecule at both levels of translation initiation efficiency demonstrate that there was no accumulation of degradation intermediates.

Premature termination of translation elongation destabilizes the mRNA evenly throughout the coding and the ribosome-free regions, and decreases local mRNA concentrations after the stop codon

To study the effect of the number of ribosomes in translation on the stability and concentration of mRNA without changing their density on the CDS, we constructed a series of mRNAs with similar translation initiation but shortened *lacZ* coding sequences. By inserting an internal stop codon (UAG amber codon), we generated mRNAs with 75, 50, 25 and 0.5% of the initial *lacZ* CDS length (Figure 3) and hybrid ribosome coverage, i.e. partly translated up to the inserted stop codon with the rest of the molecule free of ribosomes. As expected, these mRNAs with a truncated CDS produced shortened and inactive forms of β -galactosidase (Supplementary Figure S3). Polysome profiling experiments revealed that regardless of their *lacZ* CDS length, only a small proportion of the mRNAs were ribosome free (fraction A), showing that most mRNAs were engaged in translation, as expected since the efficiency of translation initiation was not altered. The mRNAs with full-length and 75%-length *lacZ* CDSs were heavily ribosome loaded, with a majority carrying >8 ribosomes per

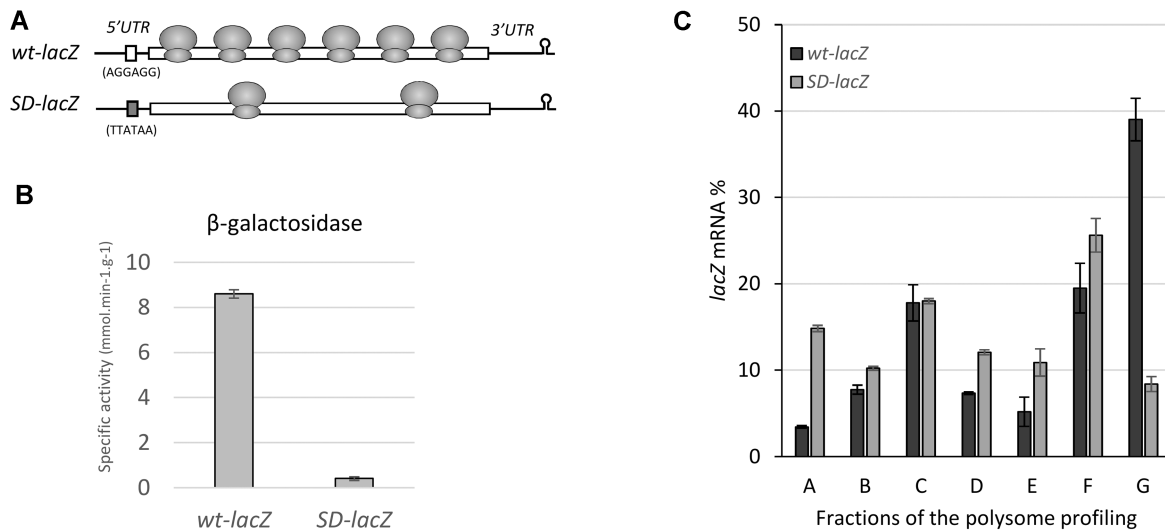


Figure 1. Reducing the efficiency of translation initiation decreased β -galactosidase activity and the proportion of translated *lacZ* mRNAs. (A) Schematic representation of *wt-lacZ*, the reference mRNA with efficient translation initiation, and *SD-lacZ*, an mRNA molecule with reduced translation initiation efficiency. The latter is loaded with fewer ribosomes as a result. The two SD sequences are highlighted and their sequence is indicated. 3'-UTRs are identical and contain the *rrnB* transcriptional terminator. (B) β -Galactosidase activity measured for *wt-lacZ*- and *SD-lacZ*-containing strains. Error bars represent standard deviations ($n = 9$, three biological and three technical replicates). (C) Distributions of ribosome loads on *wt-lacZ* (dark grey) and *SD-lacZ* (light grey) mRNAs. Fraction A consists of free mRNA molecules, while fractions B–G consist of mRNA molecules in translation with B, 1.1 ± 0.1 ; C, 2.8 ± 0.3 ; D, 4.7 ± 0.4 ; E, 5.9 ± 0.5 ; F, 8.2 ± 0.6 ; and G, 11.4 ± 0.4 bound ribosomes per mRNA molecule (24). The percentages in each fraction correspond to the proportions of the total amount of mRNA measured in that fraction. Error bars represent the standard deviations of two technical replicates. The polysome profiles are provided in Supplementary Figure S4.

molecule (in fractions F and G). With shorter CDSs, the ribosome loads shifted to lighter fractions with predominantly 4–6 ribosomes for *lacZ*-Stop_{50%} and 1–3 ribosomes for *lacZ*-Stop_{25%} and *lacZ*-Stop_{0.5%} (i.e. the most populated fractions were D and E, and B and C, respectively).

The local half-lives of the different *lacZ*-Stop mRNAs were measured using primers distributed along the molecule and on either side of the inserted stop codon (Figure 4A). The transcripts with shortened *lacZ* CDSs were destabilized homogeneously along the full length of the molecule [Figure 4B; the data from the mRNA with a full-length *lacZ* CDS (Figure 2B) are shown again for comparison] resulting in average half-lives of ~ 1 min, regardless of the extent of the CDS reduction (Figure 4C). This means that the local stability was similar in the ribosome-covered and ribosome-free parts of the mRNA molecule. Furthermore, no major differences in local stability were observed between predominantly translated molecules (*lacZ*-Stop_{75%}) and those that were essentially untranslated (*lacZ*-Stop_{0.5%}). The absence of a correlation between the level of destabilization and the length of the untranslated portion suggests that it is simply the presence of an untranslated portion of mRNA that destabilizes the transcript, regardless of the length of this portion. The similarity of the local half-lives suggests once more that no degradation intermediates accumulated in the cells.

Figure 4D shows the effects of a premature termination of translation elongation on local mRNA concentrations with 75, 50 and 25% of the initial *lacZ* CDS. For all the constructs, a decrease in local mRNA concentrations downstream of the stop codon is observed. Insertion of the stop codon displaced this decrease in local mRNA concentra-

tions. The local concentrations in the untranslated parts level off at $\sim 5\%$ of the concentrations measured at the 5' end. Since the local half-lives were similar upstream and downstream of the internal stop codon (Figure 4B), the decrease in local concentrations after the stop codon cannot be attributed to a difference in stability between the translated and untranslated parts of the mRNA. Instead, uncoupling of transcription and translation shortly after the internal stop codon could explain the drop in downstream mRNA concentrations through a partial premature arrest of transcription elongation (7). To confirm this hypothesis, we restored the coupling between translation and transcription using an orthogonal translation system capable of translating the internal amber stop codon and resuming protein synthesis (Figure 5A) (38). Aligned with the amplicon positions along the molecules (Figure 5B), Figure 5C shows that when translation was restored at the internal stop codon (*lacZ*-Stop_{50%}-tRNA_o), the local mRNA concentrations no longer decreased downstream of the stop codon. This result confirms that the drop in local mRNA concentrations downstream of the internal stop codon is due to uncoupling between translation and transcription.

Removing the untranslated region restabilizes the whole mRNA molecule

The presence of a UTR destabilizes the whole *lacZ* mRNA molecule and the level of destabilization is not proportional to the length of the UTR. To confirm the destabilizing effect of the UTRs, we generated a new set of *lacZ* mRNAs without these regions (Figure 6A). These new constructs (*lacZ*_{75%} Δ , *lacZ*_{50%} Δ and *lacZ*_{25%} Δ) had identical 5'- and

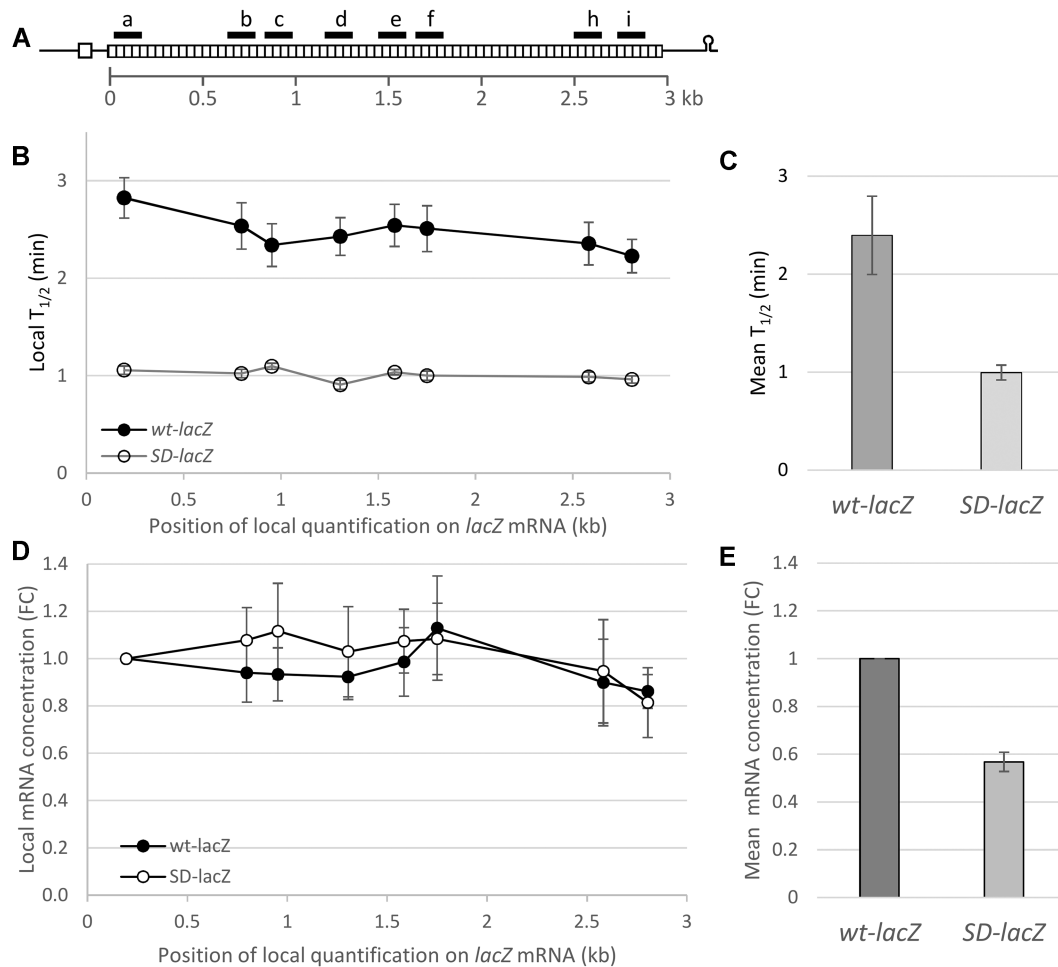


Figure 2. Decreasing the efficiency of translation initiation destabilizes the *lacZ* mRNA and leads to a uniform decrease in mRNA concentration throughout the molecule. (A) Schematic representation of *lacZ* mRNA with the CDS shown as a striped rectangle. The black marks with letters indicate the amplicons used for qRT-PCR quantification, with their position on the mRNA measured relative to the first codon of the CDS (scale in kb, values given in the Materials and Methods). The white square at the 5' end represents the SD sequence (AGGAGG for *wt-lacZ*, TAATTA for *SD-lacZ*). (B) Local *lacZ* mRNA stability. Local half-lives ($T_{1/2}$) were determined at different positions using different primer pairs (qPCR amplicon locations are shown on the above scheme). Error bars denote standard deviations ($n = 5-10$). (C) Mean half-life of the entire *lacZ* mRNA molecule for *wt-lacZ* and *SD-lacZ*. Error bars represent standard deviations ($n = 40-80$). (D) Local *lacZ* mRNA concentration. The local *lacZ* mRNA concentration was measured at different positions using different primer pairs by qRT-PCR and is expressed as an FC relative to the concentration measured for amplicon 'a'. Error bars represent standard deviations ($n = 6$). (E) Mean mRNA concentration of entire *lacZ* mRNA molecules. The concentration of *SD-lacZ* is expressed as an FC relative to the concentration of *wt-lacZ*. Error bars denote standard deviations ($n = 8$).

3'-UTRs and either 75, 50 or 25% of the initial *wt-lacZ* CDS.

All mRNAs showed a similarly constant local stability profile, independent of the length of the remaining CDS region and close to the profile measured for the full-length *lacZ* CDS of the *wt-lacZ* strain (Figure 6B). This means that removing the untranslated portion of the CDS increased the mRNA half-lives from 1 min on average (Figure 4C) to 2–2.6 min (Figure 6C), similar to the values measured for the full-length CDS of the *wt-lacZ* strain (Figure 6C). We can conclude that the destabilization of transcripts with an inserted stop codon was driven by the untranslated part of the CDS.

Local mRNA concentrations decreased slightly in the portion corresponding to the *lacZ* CDS region for all constructs (Figure 6D). These decreasing trends are similar to those observed upstream of the stop codon in the con-

structs with the UTR still in place (Figure 4D). However, the mRNA concentrations measured at the 5' end were higher in the constructs without the UTRs (compare Figures 4E and 6E).

These results show that removing the untranslated portion of the *lacZ* CDS region restores the stability of the mRNA and the concentration of its 5' end relative to those of full-length *lacZ* CDS. After premature termination of translation elongation, it is therefore the presence of a UTR (of any length) that destabilizes the whole mRNA molecule and leads to a decrease in concentration at the 5' end. However, a decrease in local concentrations upstream of the inserted stop codon was still observed after removing the untranslated part of the *lacZ* CDS region. Because there were no local variations in mRNA stability, we can speculate that the variations in local concentrations observed may instead be related to differences in transcription. Differences

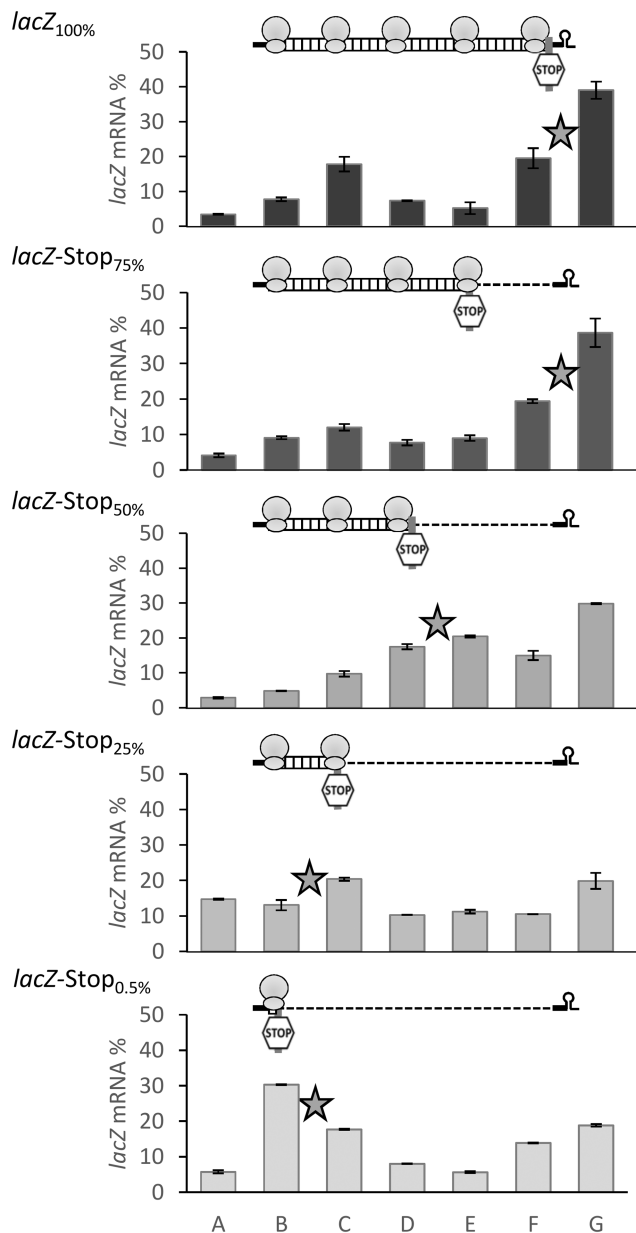


Figure 3. Premature termination of translation elongation shifts *lacZ* mRNA from ribosome-heavy fractions to lighter fractions. Ribosome distributions on *lacZ* mRNAs with 100% to 0.5% of the CDS. mRNA-ribosome complexes were fractionated on a sucrose gradient; total mRNAs were then purified and *lacZ* mRNA quantified in each fraction. Fraction A consists of free mRNA molecules, while fractions B–G consist of mRNA molecules in translation bound with B, 1.1 ± 0.1 ; C, 2.8 ± 0.3 ; D, 4.7 ± 0.4 ; E, 5.9 ± 0.5 ; F, 8.2 ± 0.6 ; and G, 11.4 ± 0.4 bound ribosomes per mRNA molecule (24). The percentages in each fraction correspond to the proportions of the total amount of mRNA measured in that fraction. Error bars represent the standard deviation of two technical replicates. A schematic representation of the construct for each strain is shown above each graph, with translating ribosomes above the CDS drawn as a striped rectangle, and the untranslated part after the inserted stop codon represented by a dashed line. The large star indicates the two consecutive fractions with the largest combined amount of *lacZ* mRNA. The polysome profiles are provided in Supplementary Figure S5.

in transcription could also explain the drop in local concentrations downstream of the inserted stop codon when the untranslated portion of the *lacZ* CDS region is present (Figure 4D), while the level of destabilization is uniform throughout the molecule (Figure 4B).

The RNase E activity of an assembled RNA degradosome is involved in the destabilization of partially translated mRNAs

Since RNase E cleavage is considered the initial step of RNA degradation in *E. coli*, we analysed the role of RNase E in destabilizing a partially translated *lacZ* transcript. The two forms *wt-lacZ* and *lacZ-Stop_{50%}* (Figure 7A) were expressed in the genetic background of MC1061 carrying a thermosensitive (RNase E Ts) or control (RNase E wt) version of RNase E (31). In the presence of RNase E wt, the homogeneous destabilization of *lacZ-Stop_{50%}* relative to *wt-lacZ* was confirmed (Figure 7B) showing that the destabilization of *lacZ-Stop_{50%}* (also observed in MG1655, Figure 4B) is independent of genetic background. Inactivation of RNase E activity by shifting the cultures to 42°C resulted in the very strong stabilization of *wt-lacZ* mRNA (half-lives >6 min in Figure 7C compared with 1.6 min with RNase E wt in Figure 7B). The dependence on *lacZ* mRNA stability of RNase E activity is consistent with the literature (40). The *lacZ-Stop_{50%}* mRNA was also stabilized with RNase E Ts at 42°C (Figure 7C): the region upstream of the inserted stop codon was stabilized by a factor of 2 (half-lives of 2 min versus 1 min) whereas the downstream region was stabilized up to 10-fold (Figure 7C, amplicons g–i). These results show that RNase E activity is involved in the destabilization of the partially translated *lacZ-Stop_{50%}* mRNA. The fact that half-lives of *lacZ-Stop_{50%}* mRNA were lower than those of *wt-lacZ* mRNA with RNase E Ts could be related to the activities of other degradation enzymes. These activities could also be responsible for the differential stability of *lacZ-Stop_{50%}* mRNA upstream and downstream of the stop codon.

The C-terminal region of RNase E is a scaffold for the formation of RNA degradosomes (32). The above results show that it is the activity of RNase E bound to the RNA degradosome that contributes to the destabilization of *lacZ-Stop_{50%}* mRNA. We thus wondered whether the formation of the RNA degradosome was necessary for the destabilization of *lacZ-Stop_{50%}* by RNase E. The *wt-lacZ* and *lacZ-Stop_{50%}* mRNAs (Figure 8A) were expressed in KSL2000 strains containing control RNase E wt able to form the RNA degradosome and truncated RNase E Δ Cter unable to form the RNA degradosome, respectively (32). In the presence of the RNA degradosome (RNase E wt), uniform destabilization of *lacZ-Stop_{50%}* was again observed in the KSL2000 genetic background (Figure 8B). In the absence of the RNA degradosome (RNase E Δ Cter), *lacZ-Stop_{50%}* mRNA was also stabilized, although only the half-life of the region downstream of the stop codon reached the half-life of *wt-lacZ* (Figure 8C). These results show that an assembled RNA degradosome is required for destabilization of the *lacZ-Stop_{50%}* UTR by RNase E.

The RNA degradosome localizes to the inner membrane by the MTS domain of RNase E (32). We used a KSL2000 strain expressing a cytoplasmic RNA degradosome (RNase

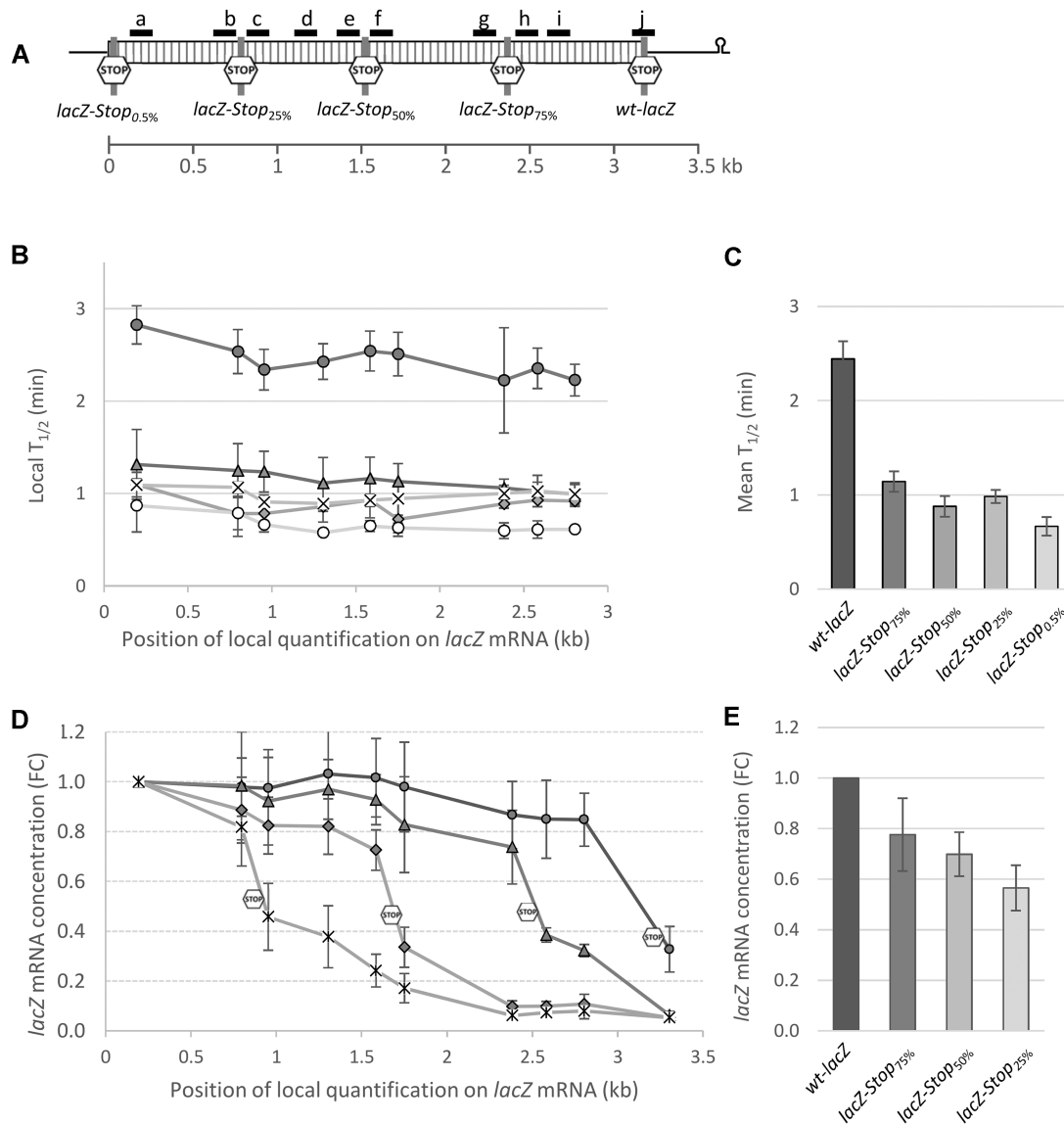


Figure 4. Premature termination of translation elongation uniformly destabilizes the mRNA and decreases local mRNA concentrations after the stop codon. (A) Schematic representation of the analysed *lacZ* mRNAs, with the positions of the stop codon and the proportions of the CDS relative to *wt-lacZ* indicated. The black marks and letters indicate the amplicons used for qRT-PCR quantification. The scale corresponds to the number of *lacZ* mRNA bases (in kb) relative to the start codon. Exact coordinates are given in the Materials and Methods. (B) Local *lacZ* mRNA stability. Local half-lives ($T_{1/2}$) were determined for mRNA with a full-length *lacZ* CDS (filled circles), 75% (filled triangles), 50% (filled diamonds), 25% (crosses) or 0.5% (open circles) of the original CDS. The *x*-axis is aligned with (A). Error bars are standard deviations ($n = 10$). (C) Mean half-lives of entire *lacZ* mRNA molecules for *wt-lacZ* and *SD-lacZ*. Error bars represent standard deviations ($n = 9$). (D) Local *lacZ* mRNA concentrations were measured for molecules with a full-length *lacZ* CDS (filled circles), 75% (filled triangles), 50% (filled diamonds) or 25% (crosses) of the original CDS. The *x*-axis is aligned with (A). Changes in local mRNA concentrations are expressed as intramolecular FCs relative to the 5' end of the molecule (using amplicon 'a'). Error bars represent standard deviations ($n = 5-10$). The STOP logos represent the position of the stop codon in the molecule. (E) mRNA concentration of *lacZ* mRNAs. Concentrations were determined using amplicon 'a' and expressed as FCs relative to *wt-lacZ*. Error bars correspond to standard deviations ($n = 12-20$).

E Δ MTS) to assess whether localization of the RNA degradosome to the inner membrane was required for destabilization of *lacZ-Stop*_{50%} mRNA by RNase E. Figure 8D shows that destabilization of *lacZ-Stop*_{50%} mRNA was present even when the RNA degradosome was detached from the inner membrane, demonstrating that localization of the RNA degradosome to the inner membrane is not required for destabilization of *lacZ-Stop*_{50%} mRNA by RNase E.

Taken together, these results show that the uniform destabilization of an mRNA with a stop codon inserted in the

middle of the CDS required the RNase E activity of an assembled RNA degradosome that may or may not be localized to the inner membrane.

DISCUSSION

In the context of understanding the role of mRNA degradation and of its interactions with other cellular processes in the regulation of gene expression, we investigated how translation affects mRNA stability and concentration

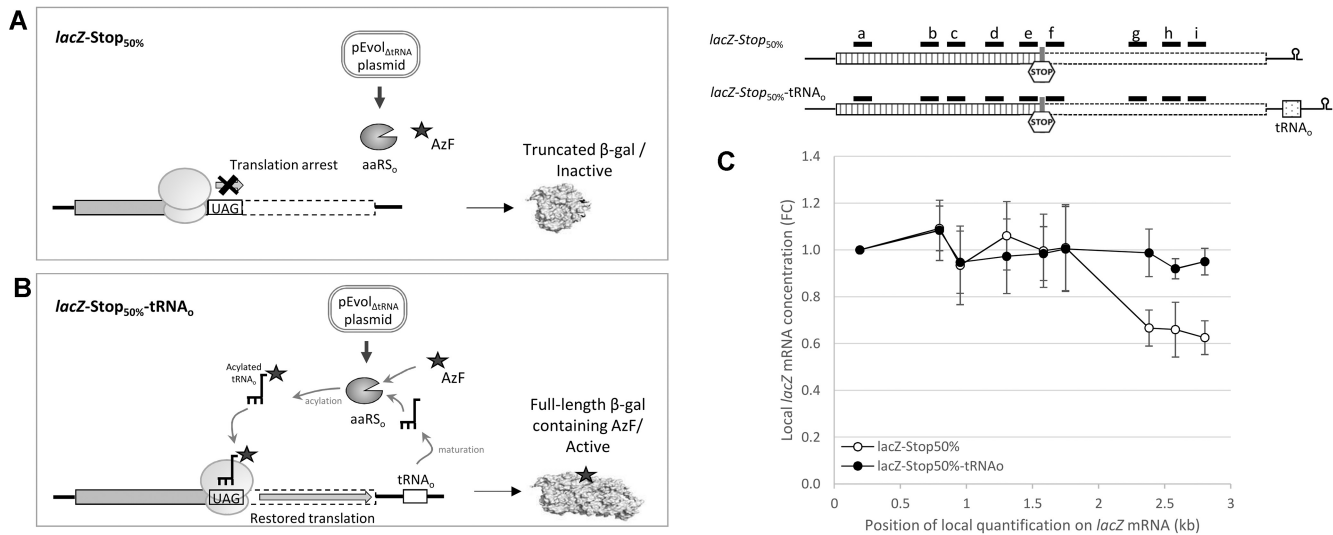


Figure 5. Translation restoration at the internal stop codon increases local mRNA concentrations after the stop codon. (A) Schematic representation of the system used. The orthogonal tRNA synthetase (aaRS₀) is expressed from a derivative of a pEvol plasmid in which the tRNA was deleted. The aaRS₀ acylated the tRNA₀ with the non-canonical amino acid AzF (black star) provided in the culture. In the upper panel (*lacZ-Stop_{50%}*), the CDS is reduced by half by the inserted amber stop codon. Ribosomes translate a truncated and inactive form of the protein. In the second panel, representing *lacZ-Stop_{50%}-tRNA₀*, tRNA₀ is expressed from the transcriptional fusion with the *lacZ-Stop_{50%}* CDS and acylated with AzF by the aaRS₀. Ribosomes can then load AzF-tRNA₀ to decode the amber codon UAG and continue translation to produce a full-length active protein containing AzF. (B) Schematic representation of the positions of the qPCR amplicons. Amplicons 'a' to 'i' were used for both *lacZ-Stop_{50%}* and *lacZ-Stop_{50%}-tRNA₀*. (C) Local mRNA concentrations were measured for *lacZ-Stop_{50%}* (open circles) and *lacZ-Stop_{50%}-tRNA₀* (filled circles). The location of the measurements is shown relative to their positions along the mRNA (in kb). Concentrations are expressed as FCs relative to the values measured with amplicon 'a'. Error bars represent standard deviations ($n = 5-10$).

through measuring local stabilities and local concentrations all along the molecule. To our knowledge, local stability measurements have never previously been included in studies of mRNA degradation. This intramolecular mapping provides more detailed information on transcript behaviour in the presence of translational perturbations. Reducing the efficiency of translation initiation and prematurely terminating translation elongation were both observed to destabilize the transcript from end to end. The fact that stability decreased uniformly indicates that there was no accumulation of specific degradation products. Northern blot quantifications of *lacZ* mRNA stability have likewise shown no accumulation of intermediates or smears (40,41). The absence or non-detection of decay intermediates can be explained in several ways. It may be that the degradation fragments are degraded too rapidly. After initial internal endonucleolytic cleavage, the increased activity of RNase Es towards monophosphorylated 5' ends (42) may lead to rapid processing of the fragment with a newly generated 5' end, while the newly generated 3' end can be rapidly processed by 3' exoribonucleases such as PNPase and RNase II because it does not have the protective secondary structure usually present at the 3' end of full-length transcripts (43). This explanation assumes that the limiting step in the degradation process is the initial internal cleavage and that the intermediates decay extremely rapidly (44). A second plausible explanation for the non-accumulation of decay intermediates is that a large set of heterogeneous fragments generated by randomly distributed initial cleavages cover the whole mRNA molecule. In support of this hypothesis, Herzal *et al.* (45) recently showed that a large fraction of cel-

lular RNA consists of decay fragments with 3' ends widely distributed across internal positions in the transcript. This explanation implies that the stability of any decay fragment does not exceed the stability of the full-length transcript. Finally, it cannot be excluded that some fragments accumulated but were not detected because they were not targeted by our qRT-PCR approach. We consider this explanation unlikely, however, since we quantified up to 10 different mRNA regions widely distributed throughout the molecule.

From a mechanistic point of view, our results showed that RNase E is a determinant of the stability of fully translated and partially translated mRNAs (*wt-lacZ* and *lacZ-Stop_{50%}*, respectively) because they are stabilized in the absence of RNase E activity. Stabilization of partially translated mRNAs was more pronounced in the UTR than for the translated region, suggesting that the absence of ribosomes facilitates direct RNase E entry. The fact that the stabilization of *lacZ-Stop_{50%}* mRNA was lower than that of *wt-lacZ* mRNA in the absence of RNase E activity indicates that other degradation enzymes contribute to the destabilization of partially translated mRNAs. The ribosome-free region could also facilitate access to the other endonucleolytic enzyme, RNase III, since six potential stem-loop structures with $\Delta G < -10$ kcal/mol are detected in this region. After cleavage by RNase E and/or RNase III in the ribosome-free region, the newly formed fragments, lacking the protective secondary structures at the 3' end, will be degraded by 3'-5' exonucleases such as PNPase or RNase II. We also demonstrated that destabilization of *lacZ-Stop_{50%}* mRNA by RNase E required the formation of the RNA degradosome, at the inner membrane or not. The weak

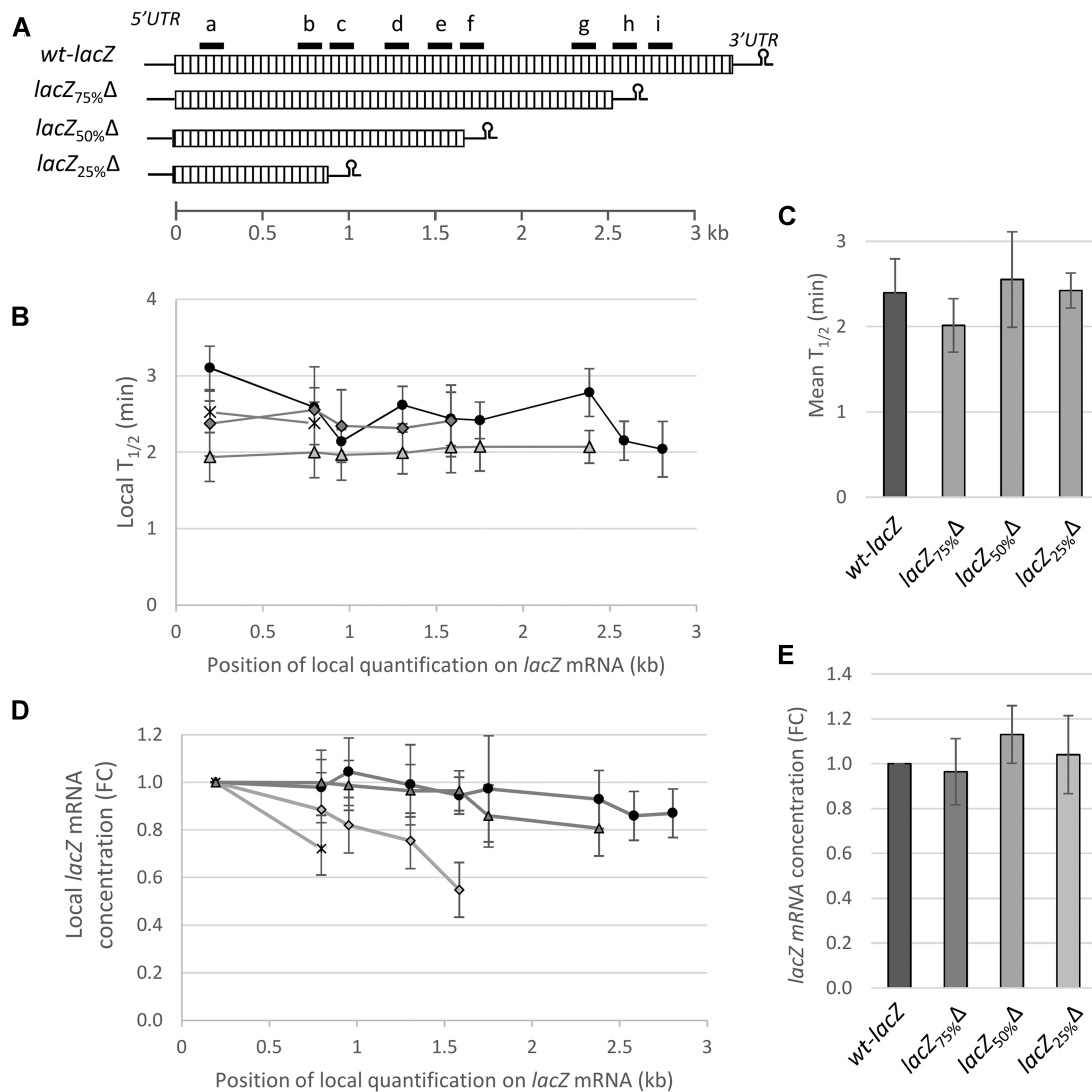


Figure 6. Removing the UTR restabilizes the whole *lacZ* mRNA molecule. (A) Schematic representation of *lacZ* mRNAs with different CDS lengths. The black marks and letters indicate the amplicons used for qRT-PCR measurements. The scale corresponds to the number of *lacZ* mRNA bases (in kb) relative to the start codon. Exact coordinates are given in the Materials and Methods. (B) Local *lacZ* mRNA stability. Local half-lives ($T_{1/2}$) were measured using primer pairs located along the constructs represented in (A): wt-*lacZ* (circles), *lacZ*_{75%Δ} (triangles), *lacZ*_{50%Δ} (diamonds) and *lacZ*_{25%Δ} (crosses). Error bars correspond to standard deviations ($n = 4-10$). (C) Mean half-lives of the *lacZ* mRNA molecules. The values shown are the averages of all measurements with each pair of primers for the corresponding *lacZ* variant. Error bars represent standard deviations ($n = 8-45$). (D) Local *lacZ* mRNA concentrations were measured for full-length wt-*lacZ* CDS (filled circles) and the constructs represented in (A): *lacZ*_{75%Δ} (filled triangles), *lacZ*_{50%Δ} (filled diamonds) and *lacZ*_{25%Δ} (crosses). The x-axis is aligned with (A). Concentrations are expressed as FCs relative to the concentration measured with amplicon 'a'. Error bars represent standard deviations ($n = 5-10$). (E) Relative *lacZ* mRNA concentrations determined using the 'a' amplicon and expressed as FCs relative to wt-*lacZ*. Error bars represent standard deviations ($n = 6-18$).

effect of RNA degradosome detachment from the inner membrane on *lacZ*-Stop_{50%} mRNA stability is consistent with previous omics studies showing that RNA degradosome detachment from the inner membrane had a moderate stabilizing effect (16,46) and did not significantly affect the *lacZ* mRNA half-life (16). The requirement of degradosome assembly for *lacZ*-Stop_{50%} mRNA destabilization by RNase E suggests that at least one RNA degradosome component contributes to the RNase E-dependent degradation process of partially translated mRNAs. Candidates could be RhlB, which was shown to facilitate RNase E cleavage of ribosome-free mRNA (32), or PN-

Pase, whose 3'-5' exonuclease activity degrades fragments generated by RNase E cleavage. Further studies are needed to identify the components of the RNA degradosome and the underlying mechanisms that contribute with RNase E to the specific degradation of improperly translated transcripts.

Our study also specifically investigated the role of ribosomes in linking translation and mRNA degradation. Reducing translation initiation efficiency was found to reduce the number of bound ribosomes and the stability of the entire mRNA molecule. These results confirm the protective effect of ribosomes when translation initiation is

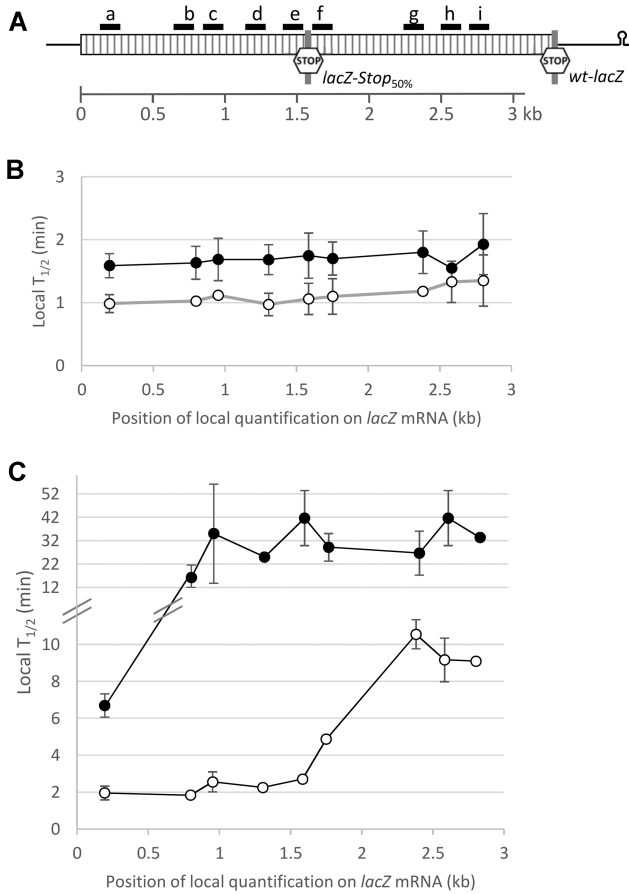


Figure 7. RNase E activity is responsible for $lacZ-Stop_{50\%}$ destabilization. (A) Schematic representation of $wt-lacZ$ and $lacZ-Stop_{50\%}$ mRNAs, with black marks and letters indicating the amplicons used for qRT-PCR measurements. The scale corresponds to the number of $lacZ$ mRNA bases (in kb) relative to the start codon. (B) Local $wt-lacZ$ (filled circles) and $lacZ-Stop_{50\%}$ (open circles) mRNA stability in the RNase E wt context. Local half-lives ($T_{1/2}$) were measured using primer pairs located along the constructs. Error bars correspond to standard deviations ($n = 2$). (C) Local $wt-lacZ$ (filled circles) and $lacZ-Stop_{50\%}$ (open circles) mRNA stability in the RNase E TS variant. Local half-lives ($T_{1/2}$) were measured using primer pairs located along the constructs. Error bars correspond to standard deviations ($n = 2$).

efficient, probably by preventing 5' end-dependent degradation by RNase E (5,6), which extends the protective effect to the whole molecule. In the case of premature termination of translation elongation, our results show that the presence of an untranslated portion, regardless of its length, destabilizes the whole mRNA molecule. This also suggests that ribosomes have a protective effect, in this case probably through steric hindrance of RNase E action. Ribosomes have been reported to destabilize transcripts when they become stalled on the transcript or when they elongate slowly (5,6). Here, the same half-lives were measured for the ribosome-covered translated regions and the ribosome-free UTRs of the mRNA, suggesting no destabilizing effect; however, this was expected because the internal stop codon arrested translation and induced ribosome drop-off rather than stalling the ribosome or altering the rate of upstream ribosome elongation.

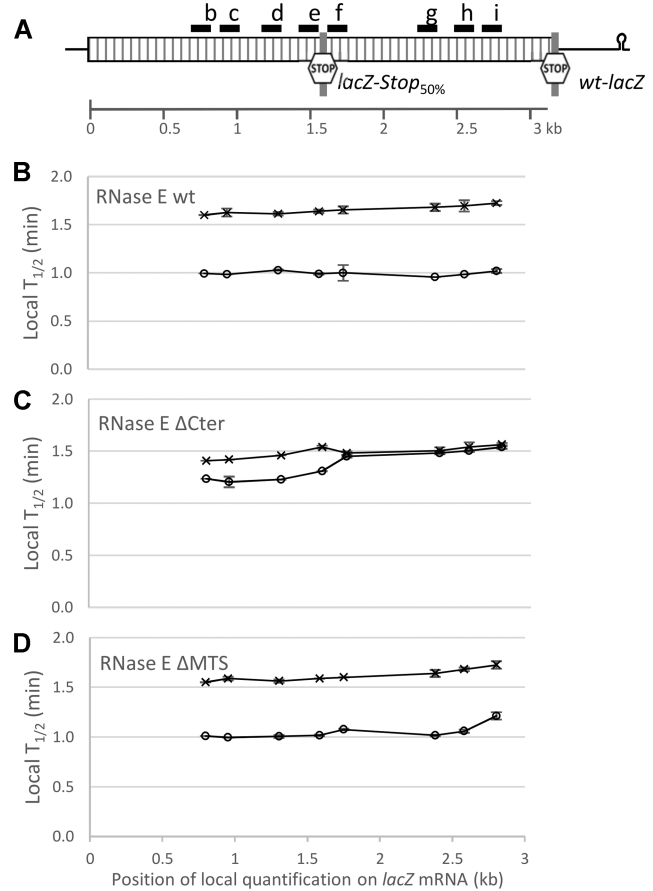


Figure 8. Degradosome formation but not RNase E localization is responsible for $lacZ-Stop_{50\%}$ mRNA destabilization. (A) Schematic representation of $wt-lacZ$ and $lacZ-Stop_{50\%}$ mRNAs, with black marks and letters indicating the amplicons used for qRT-PCR measurements. The scale corresponds to the number of $lacZ$ mRNA bases (in kb) relative to the start codon. Local $wt-lacZ$ (crosses) and $lacZ-Stop_{50\%}$ (filled circles) mRNA half-lives were measured in KSL2000 derivative strains expressing wt -RNase E (B), RNase E $\Delta Cter$ (C) or RNase E ΔMTS (D). Quantification points are aligned with amplicons used (A). Error bars correspond to standard deviations ($n = 2$).

Regarding transcription, when the whole mRNA molecule was destabilized by inefficient translation initiation, this did not strongly affect transcription; however, transcription was affected when the mRNA was destabilized by premature termination of translation elongation. Uncoupling of transcription and translation downstream of the internal stop codon induced a sharp downstream decrease in mRNA concentrations due to Rho-dependent premature termination of transcription elongation (7). However, our results indicate that the coupling of transcription and translation is not an all-or-nothing mechanism. A minority of transcription elongation events leading to complete $lacZ$ CDS transcription (Figure 4D) were effective even when transcription and translation were decoupled. This was also confirmed by the expression of functional $tRNA_{\text{A}}$ molecules transcribed from the 3' end of the mRNA and able to restore translation at an amber stop codon. Conversely, the fact that local mRNA concentrations (but not mRNA stability) decreased slightly upstream

of the inserted stop codon (Figure 4B, D) suggests that even when translation and transcription are coupled, a fraction of transcription events do not lead to the synthesis of the full-length transcript. This appears to be independent of the presence or absence of a UTR (Figures 4D and 6D). This premature termination of transcription could generate heterogeneity in the transcript population. Further studies are required to explore this hypothesis.

The coordination of the three processes of transcription, translation and mRNA degradation is essential for proper cell functioning and constitutes a first line of translation quality control. In eukaryotes, the first round of translation by a pioneer ribosome was proposed to serve as an mRNA quality control of aberrant mRNAs carrying premature termination codons that can potentially generate toxic truncated proteins (47,48). The detection of premature stop codons by the pioneer ribosome leads to mRNA degradation through the mechanism known as nonsense-mediated decay. In bacteria, transcription is not an error-free event, with an estimated ribonucleotide misincorporation frequency in *E. coli* of 5×10^{-5} to 5×10^{-6} per nucleotide (49,50). In ~4% of cases, misincorporation results in the appearance of stop codons (49) and the production of defective proteins that can impair cellular integrity and fitness. This can be particularly deleterious for poorly transcribed genes with only a few mRNA molecules available in the cell to ensure translation. Removing non-productive translation templates is particularly important for the cell in these cases. For the first time we have shown the role of RNase E activity and degradosome formation in this quality control process. As soon as a coupling defect appears, cells respond by rapidly degrading the corrupted mRNA by RNase E.

In conclusion, this study provides new evidence on the close relationship between the degradation of an mRNA molecule and its translational state. Low ribosome density or the presence of a ribosome-free region destabilizes the entire mRNA molecule. Overall destabilization leads to an overall decrease in concentration, while changes in transcription lead to local differences in concentration along the mRNA molecule. Quality control and mRNA concentrations are therefore governed by the interplay of the transcription–translation–mRNA degradation triarchy. This *ménage à trois* is a centrally coordinated mechanism that shapes gene expression in bacteria.

DATA AVAILABILITY

The data underlying this article are available in the article and in its online supplementary material.

SUPPLEMENTARY DATA

[Supplementary Data](#) are available at NAR Online.

ACKNOWLEDGEMENTS

The authors thank M. Audonnet and P. Lopez for technical support, and A.J. Carpousis for comments on the manuscript and the kind gift of RNase E mutant strains used in this study.

Authors contributions: S.N. and L.G. conceived the study. F.C. produced the constructs and analysed the modified translation initiation data. M.P.D. performed part of the stability analysis and all the polysome profiling experiments. S.N. performed all other experiments. S.N., L.G. and M.C.B. contributed equally to the preparation and writing of the manuscript.

FUNDING

This study was carried out on the BLADE (Bacterial Adaptation, Diversity and Engineering) team's own funds. *Conflict of interest statement.* None declared.

REFERENCES

- Mohanty, B.K. and Kushner, S.R. (2016) Regulation of mRNA decay in bacteria. *Annu. Rev. Microbiol.*, **70**, 25–44.
- Callaghan, A.J., Aurikko, J.P., Ilag, L.L., Günter Grossmann, J., Chandran, V., Kühnel, K., Poljak, L., Carpousis, A.J., Robinson, C.V., Symmons, M.F. *et al.* (2004) Studies of the RNA degradosome-organizing domain of the *Escherichia coli* ribonuclease RNase E. *J. Mol. Biol.*, **340**, 965–979.
- Carpousis, A.J. (2007) The RNA degradosome of *Escherichia coli*: an mRNA-degrading machine assembled on RNase E. *Annu. Rev. Microbiol.*, **61**, 71–87.
- Anderson, K.L. and Dunman, P.M. (2009) Messenger RNA turnover processes in *Escherichia coli*, *Bacillus subtilis*, and emerging studies in *Staphylococcus aureus*. *Int. J. Microbiol.*, **2009**, 525491.
- Deana, A. and Belasco, J.G. (2005) Lost in translation: the influence of ribosomes on bacterial mRNA decay. *Genes Dev.*, **19**, 2526–2533.
- Dreyfus, M. (2009) Killer and protective ribosomes. *Prog. Mol. Biol. Transl. Sci.*, **85**, 423–466.
- Zhu, M., Mori, M., Hwa, T. and Dai, X. (2019) Disruption of transcription–translation coordination in *Escherichia coli* leads to premature transcriptional termination. *Nat. Microbiol.*, **4**, 2347–2356.
- Yarchuk, O., Iost, I. and Dreyfus, M. (1991) The relation between translation and mRNA degradation in the *lacZ* gene. *Biochimie*, **73**, 1533–1541.
- Cambray, G., Guimaraes, J.C. and Arkin, A.P. (2018) Evaluation of 244,000 synthetic sequences reveals design principles to optimize translation in *Escherichia coli*. *Nat. Biotechnol.*, **36**, 1005–1015.
- Kosuri, S., Goodman, D.B., Cambray, G., Mutalik, V.K., Gao, Y., Arkin, A.P., Endy, D. and Church, G.M. (2013) Composability of regulatory sequences controlling transcription and translation in *Escherichia coli*. *Proc. Natl Acad. Sci. USA*, **110**, 14024–14029.
- Pedersen, S., Terkelsen, T.B., Eriksen, M., Hauge, M.K., Lund, C.C., Sneppen, K. and Mitarai, N. (2019) Fast translation within the first 45 codons decreases mRNA stability and increases premature transcription termination in *E. coli*. *J. Mol. Biol.*, **431**, 1088–1097.
- Boël, G., Letso, R., Neely, H., Price, W.N., Wong, K.H., Su, M., Luff, J., Valecha, M., Everett, J.K., Acton, T.B. *et al.* (2016) Codon influence on protein expression in *E. coli* correlates with mRNA levels. *Nature*, **529**, 358–363.
- Esquerré, T., Moisan, A., Chiapello, H., Arike, L., Vilu, R., Gaspin, C., Coccagn-Bousquet, M. and Girbal, L. (2015) Genome-wide investigation of mRNA lifetime determinants in *Escherichia coli* cells cultured at different growth rates. *BMC Genomics*, **16**, 275.
- Tsai, Y.C., Du, D., Domínguez-Malfavón, L., Dimastrogiovanni, D., Cross, J., Callaghan, A.J., García-Mena, J. and Luisi, B.F. (2012) Recognition of the 70S ribosome and polysome by the RNA degradosome in *Escherichia coli*. *Nucleic Acids Res.*, **40**, 10417–10431.
- Hamouche, L., Poljak, L. and Carpousis, A.J. (2021) Polyribosome-dependent clustering of membrane-anchored RNA degradosomes to form sites of mRNA degradation in *Escherichia coli*. *Mbio*, **12**, e0193221.
- Hadjeras, L., Poljak, L., Bouvier, M., Morin-Ogier, Q., Canal, I., Coccagn-Bousquet, M., Girbal, L. and Carpousis, A.J. (2019) Detachment of the RNA degradosome from the inner membrane of *Escherichia coli* results in a global slowdown of mRNA degradation, proteolysis of RNase E and increased turnover of ribosome-free transcripts. *Mol. Microbiol.*, **111**, 1715–1731.

17. Fan, H., Conn, A.B., Williams, P.B., Diggs, S., Hahm, J., Gamper, H.B. Jr, Hou, Y.M., O'Leary, S.E., Wang, Y. and Blaha, G.M. (2017) Transcription–translation coupling: direct interactions of RNA polymerase with ribosomes and ribosomal subunits. *Nucleic Acids Res.*, **45**, 11043–11055.
18. Kohler, R., Mooney, R.A., Mills, D.J., Landick, R. and Cramer, P. (2017) Architecture of a transcribing–translating expressome. *Science*, **356**, 194–197.
19. Saxena, S., Myka, K.K., Washburn, R., Costantino, N., Court, D.L. and Gottesman, M.E. (2018) *Escherichia coli* transcription factor NusG binds to 70S ribosomes. *Mol. Microbiol.*, **108**, 495–504.
20. Iyer, S., Le, D., Park, B.R. and Kim, M. (2018) Distinct mechanisms coordinate transcription and translation under carbon and nitrogen starvation in *Escherichia coli*. *Nat. Microbiol.*, **3**, 741–748.
21. Proshkin, S., Rahmouni, A.R., Mironov, A. and Nudler, E. (2010) Cooperation between translating ribosomes and RNA polymerase in transcription elongation. *Science*, **328**, 504–508.
22. Vogel, U. and Jensen, K.F. (1994) The RNA chain elongation rate in *Escherichia coli* depends on the growth rate. *J. Bacteriol.*, **176**, 2807–2813.
23. Castellana, M., Hsin-Jung Li, S. and Wingreen, N.S. (2016) Spatial organization of bacterial transcription and translation. *Proc. Natl Acad. Sci. USA*, **113**, 9286–9291.
24. Nguyen, H.L., Duviau, M.P., Laguerre, S., Nouaille, S., Coccain-Bousquet, M. and Girbal, L. (2022) Synergistic regulation of transcription and translation in *Escherichia coli* revealed by codirectional increases in mRNA concentration and translation efficiency. *Microbiol. Spectr.*, **10**, e0204121.
25. Nouaille, S., Mondeil, S., Finoux, A.L., Moulis, C., Girbal, L. and Coccain-Bousquet, M. (2017) The stability of an mRNA is influenced by its concentration: a potential physical mechanism to regulate gene expression. *Nucleic Acids Res.*, **45**, 11711–11724.
26. Choe, D., Lee, J.H., Yoo, M., Hwang, S., Sung, B.H., Cho, S., Palsson, B., Kim, S.C. and Cho, B.-K. (2017) Adaptive laboratory evolution of a genome-reduced *Escherichia coli*. *Nat. Commun.*, **10**, 935.
27. Dressaire, C., Pobre, V., Laguerre, S., Girbal, L., Arraiano, C.M. and Coccain-Bousquet, M. (2018) PNPase is involved in the coordination of mRNA degradation and expression in stationary phase cells of *Escherichia coli*. *BMC Genomics*, **19**, 848.
28. Nguyen, H.L., Duviau, M.P., Coccain-Bousquet, M., Nouaille, S. and Girbal, L. (2019) Multiplexing polysome profiling experiments to study translation in *Escherichia coli*. *PLoS One*, **14**, e0212297.
29. Etienne, T.A., Coccain-Bousquet, M. and Ropers, D. (2020) Competitive effects in bacterial mRNA decay. *J. Theor. Biol.*, **504**, 110333.
30. Esquerré, T., Laguerre, S., Turlan, C., Carpousis, A.J., Girbal, L. and Coccain-Bousquet, M. (2014) Dual role of transcription and transcript stability in the regulation of gene expression in *Escherichia coli* cells cultured on glucose at different growth rates. *Nucleic Acids Res.*, **42**, 2460–2472.
31. Carpousis, A.J., Van Houwe, G., Ehretsmann, C. and Krisch, H.M. (1994) Copurification of *E. coli* RNAase E and PNPase: evidence for a specific association between two enzymes important in RNA processing and degradation. *Cell*, **76**, 889–900.
32. Khemici, V., Poljak, L., Luisi, B.F. and Carpousis, A.J. (2008) The RNase E of *Escherichia coli* is a membrane-binding protein. *Mol. Microbiol.*, **70**, 799–813.
33. Sambrook, J., Fritsch, E.F. and Maniatis, T. (1989) In: *Molecular Cloning: A Laboratory Manual*. Cold Spring Harbor Laboratory Press, NY.
34. Redon, E., Loubiere, P. and Coccain-Bousquet, M. (2005) Transcriptome analysis of the progressive adaptation of *Lactococcus lactis* to carbon starvation. *J. Bacteriol.*, **187**, 3589–3592.
35. Morin, M., Ropers, D., Letisse, F., Laguerre, S., Portais, J.C., Coccain-Bousquet, M. and Enjalbert, B. (2016) The post-transcriptional regulatory system CSR controls the balance of metabolic pools in upper glycolysis of *Escherichia coli*. *Mol. Microbiol.*, **100**, 686–700.
36. Spurgeon, S.L., Jones, R.C. and Ramakrishnan, R. (2008) High throughput gene expression measurement with real time PCR in a microfluidic dynamic array. *PLoS One*, **3**, e1662.
37. Pfaffl, M.W. (2001) A new mathematical model for relative quantification in real-time RT-PCR. *Nucleic Acids Res.*, **29**, e45.
38. Young, T.S., Ahmad, I., Yin, J.A. and Schultz, P.G. (2010) An enhanced system for unnatural amino acid mutagenesis in *E. coli*. *J. Mol. Biol.*, **395**, 361–374.
39. Shine, J. and Dalgarno, L. (1974) The 3'-terminal sequence of *Escherichia coli* 16S ribosomal RNA: complementarity to nonsense triplets and ribosome binding sites. *Proc. Natl Acad. Sci. USA*, **71**, 1342–1346.
40. Iost, I. and Dreyfus, M. (1995) The stability of *Escherichia coli* lacZ mRNA depends upon the simultaneity of its synthesis and translation. *EMBO J.*, **14**, 3252–3261.
41. Komarova, A.V., Tchufistova, L.S., Dreyfus, M. and Boni, I.V. (2005) AU-rich sequences within 5' untranslated leaders enhance translation and stabilize mRNA in *Escherichia coli*. *J. Bacteriol.*, **187**, 1344–1349.
42. Mackie, G.A. (1998) Ribonuclease E is a 5'-end-dependent endonuclease. *Nature*, **395**, 720–723.
43. Andrade, J.M., Pobre, V., Silva, I.J., Domingues, S. and Arraiano, C.M. (2009) The role of 3'-5' exoribonucleases in RNA degradation. *Prog. Mol. Biol. Transl. Sci.*, **85**, 187–229.
44. Carpousis, A.J., Luisi, B.F. and McDowall, K.J. (2009) Endonucleolytic initiation of mRNA decay in *Escherichia coli*. *Prog. Mol. Biol. Transl. Sci.*, **85**, 91–135.
45. Herzel, L., Stanley, J.A., Yao, C.C. and Li, G.W. (2022) Ubiquitous mRNA decay fragments in *E. coli* redefine the functional transcriptome. *Nucleic Acids Res.*, **50**, 5029–5046.
46. Moffitt, J.R., Pandey, S., Boettiger, A.N., Wang, S. and Zhuang, X. (2016) Spatial organization shapes the turnover of a bacterial transcriptome. *Elife*, **5**, e13065.
47. Maquat, L.E., Tarn, W.Y. and Isken, O. (2010) The pioneer round of translation: features and functions. *Cell*, **142**, 368–374.
48. McGlincy, N.J. and Smith, C.W. (2008) Alternative splicing resulting in nonsense-mediated mRNA decay: what is the meaning of nonsense? *Trends Biochem. Sci.*, **33**, 385–393.
49. Li, W. and Lynch, M. (2020) Universally high transcript error rates in bacteria. *Elife*, **9**, e54898.
50. Traverse, C.C. and Ochman, H. (2016) Conserved rates and patterns of transcription errors across bacterial growth states and lifestyles. *Proc. Natl Acad. Sci. USA*, **113**, 3311–3316.